

# Variation and Trend of Nitrate radical reactivity towards volatile organic compounds in Beijing, China

Hejun Hu<sup>1</sup>, Haichao Wang<sup>1,2,\*</sup>, Keding Lu<sup>3\*</sup>, Jie Wang<sup>1</sup>, Zelong Zheng<sup>1</sup>, Xuezhen Xu<sup>1</sup>, Tianyu Zhai<sup>3</sup>, Xiaorui Chen<sup>4</sup>, Xiao Lu<sup>1,2</sup>, ~~Momei Qin~~<sup>5</sup> Wenxing Fu<sup>5</sup>, Xin Li<sup>3</sup>, Limin Zeng<sup>3</sup>, Min Hu<sup>3</sup>, Yuanhang Zhang<sup>3</sup>, Shaojia Fan<sup>1,2</sup>

<sup>1</sup>School of Atmospheric Sciences, Sun Yat-sen University, and Southern Marine Science and Engineering Guangdong Laboratory (Zhuhai), Zhuhai, 519082, China

<sup>2</sup>Guangdong Provincial Observation and Research Station for Climate Environment and Air Quality Change in the Pearl River Estuary, Key Laboratory of Tropical Atmosphere-Ocean System (Sun Yat-sen University), Ministry of Education, Zhuhai, 519082, China

<sup>3</sup>State Key Joint Laboratory of Environmental Simulation and Pollution Control, The State Environmental Protection Key Laboratory of Atmospheric Ozone Pollution Control, College of Environmental Sciences and Engineering, Peking University, Beijing, 100871, China.

<sup>4</sup>Department of Civil and Environmental Engineering, The Hong Kong Polytechnic University, Hong Kong, 999077, China

<sup>5</sup>Jiangsu Key Laboratory of Atmospheric Environment Monitoring and Pollution Control, Collaborative Innovation Center of Atmospheric Environment and Equipment Technology, Nanjing University of Information Science and Technology, Nanjing, 210044, China

Correspondence to: Haichao Wang (wanghch27@mail.sysu.edu.cn), Keding Lu (k.lu@pku.edu.cn)

**ABSTRACT.** Nitrate radical ( $\text{NO}_3$ ) is an important nocturnal atmospheric oxidant in the troposphere, which significantly affects the lifetime of pollutants emitted by anthropogenic and ~~biological~~biogenic activities, especially volatile organic compounds (VOC). Here, we used one-year VOC observation data obtained in urban Beijing in 2019 to look ~~insight to~~into the level, compositions, and seasonal variation of  $\text{NO}_3$  reactivity ( $k_{\text{NO}_3}$ ). We show ~~that~~that hourly  $k_{\text{NO}_3}$  towards measured VOC highly varied from  $<10^{-4}$  to  $0.083 \text{ s}^{-1}$  with a campaign-averaged value ( $\pm$  standard deviation) of  $0.0032 \pm 0.0042 \text{ s}^{-1}$ . There was large seasonal difference in  $\text{NO}_3$  reactivity towards VOC with the average of  $0.0024 \pm 0.0026 \text{ s}^{-1}$ ,  $0.0067 \pm 0.0066 \text{ s}^{-1}$ ,  $0.0042 \pm 0.0037 \text{ s}^{-1}$ ,  $0.0027 \pm 0.0028 \text{ s}^{-1}$  from spring to winter. Alkenes such as isoprene and styrene accounted for the majority. Isoprene was the dominant species in spring, summer, and autumn, accounting for 40.0%, ~~77.2%~~77.2%, and 43.2%, respectively. Styrene only played a leading role in winter, with ~~the~~a percentage of 39.8%. ~~Sensitivity~~A sensitivity study shows monoterpenes, the species we did not measure, may account for a large fraction of  $k_{\text{NO}_3}$ . Based on the correlation between the calculated  $k_{\text{NO}_3}$  and VOC concentrations in 2019, we established localized parameterization schemes for predicting the reactivity by only using a part of VOC species. The ~~historical~~historically published VOC data was collected using the parameterization method to reconstruct the long-term  ~~$\text{NO}_3$ -reactivity~~ $k_{\text{NO}_3}$  in Beijing ~~by the parameterization method~~. The ~~downward trend of~~lower  $k_{\text{NO}_3}$  during ~~2011–2020~~2014–2021 compared with that during 2005–2013 may ~~be responded~~attribute to ~~the reduction of~~ anthropogenic VOC emission reduction. At last, we revealed

样式定义: 批注文字

样式定义: 批注框文本

样式定义: 页脚

样式定义: 页眉

样式定义: 批注主题

样式定义: EndNote Bibliography Title

样式定义: EndNote Bibliography

样式定义: 15

样式定义: 17

样式定义: 18

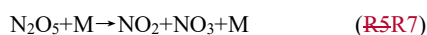
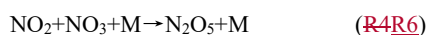
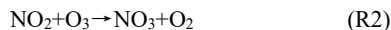
样式定义: 修订1

样式定义: 修订2

that NO<sub>3</sub> dominated the nocturnal VOC oxidation with 83% on the annual average in Beijing in 2019, which varied seasonally and was strongly regulated by the level of *k*<sub>NO<sub>3</sub></sub>, nitrogen oxide<sub>2</sub> and ozone. Our results improve the understanding of nocturnal atmospheric oxidation in urban regions, and gain the knowledge of nocturnal VOC oxidation and secondary organic pollution.

## 1. Introduction

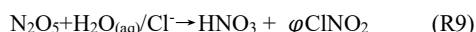
Nitrate radical (NO<sub>3</sub>) is the main nocturnal tropospheric oxidant (Brown and Stutz, 2012; Wayne et al., 1991), which is mainly formed in the reaction of NO<sub>2</sub> and O<sub>3</sub>. During the daytime, a large amount of NO emitted by cities is oxidized into NO<sub>2</sub> by ozone and released into O<sub>3</sub> in the atmosphere (R1), and NO<sub>2</sub> continues to be oxidized into nitrate radical (NO<sub>3</sub>) by O<sub>3</sub> (R2). NO<sub>3</sub> only presents a NO<sub>3</sub> is the main nocturnal tropospheric oxidant (Brown and Stutz, 2012; Wayne et al., 1991) with a relatively high concentration level at night because due to it has a rapid loss by photolysis rate (R3) and the reaction with NO during the daytime (Stark et al., 2007). NO<sub>3</sub> can oxidize NO into NO<sub>2</sub> (R3). During the nighttime, NO<sub>3</sub> and NO<sub>2</sub> react to These two reactions return NO<sub>3</sub> back to NO<sub>x</sub> and thus cannot contribute to effective NO<sub>x</sub> removal. In addition, NO<sub>3</sub> reacts with NO<sub>2</sub> to form nitrous pentoxide (N<sub>2</sub>O<sub>5</sub>) (R4R5), and N<sub>2</sub>O<sub>5</sub> can be decomposed to NO<sub>3</sub> and NO<sub>2</sub> (R5R6), establishing a temperature-dependent equilibrium.



The main removal of NO<sub>3</sub> from During the nighttime, there are two kinds of reactions that have a large impact on air pollution and regulate the lifetime and budget of many trace gas phasespecies. One is the reaction with NO (R3), solar photolysis (R6, R7), and NO<sub>3</sub> oxidizes volatile organic compounds oxidation (R8), formingand forms complex products. In addition, (R8). The other is NO<sub>3</sub> can be transformed into N<sub>2</sub>O<sub>5</sub> and removed by heterogeneous hydrolysis (R9), providing an effective way to remove NO<sub>x</sub>/NO<sub>3</sub> and produce nitrate aerosol and nitryl chloride (Brown et al., 2004; Dentener and Crutz, 1993; Osthoff et al., 2008). The competition between R8 and R9 determines the fate of nocturnal nitrogen oxidation chemistry, which leads to the formation of different type-secondary pollutants (Bertram and Thornton, 2009; Brown et al., 2006). SpecificallyIn particular, the degradation of VOC by NO<sub>3</sub>, especially biogenic VOC (Ng et al., 2017), has been proven to be related to the formation of

带格式的: 字体: Times New Roman, 小四

organic nitrate and secondary organic aerosols (SOA) (Goldstein and Galbally, 2009; Kiendler-Scharr et al., 2016).



The high  $\text{NO}_3$  concentration and fast reaction rate make  $\text{NO}_3$  responsible for the ~~sinksinking~~ of many unsaturated hydrocarbons at night (Edwards et al., 2017; Ng et al., 2017; Yang et al., 2020). The  $\text{NO}_3$  reactivity ( $k_{\text{NO}_3}$ ) towards VOC, defined as the consuming capacity of  $\text{NO}_3$  by ambient VOC, can be calculated by Eq. 1.

$$k_{\text{NO}_3} = \sum k_i \times [\text{VOC}_i] \quad \text{Eq. 1}$$

where the  $[\text{VOC}_i]$  is VOC concentrations and  $k_i$  is the corresponding reaction rate coefficients. Table S1 gives the reaction rate coefficients of  $\text{NO}_3$  with VOC (~~Atkinson and Arey, 2003~~)(Atkinson and Arey, 2003). The contribution of VOC to the  $\text{NO}_3$  reactivity ~~towardswith respect to~~ different VOC varies greatly, which is ~~affectedcaused~~ by the abundance of species and the reaction rate coefficients. Thus,  $\text{NO}_3$  reactivity towards VOC is also affected by temperature. ~~Since since~~ temperature affects not only ~~affects the~~ temperature-dependent reaction rate coefficients but also the VOC ~~concentrationsemissions~~ in the atmosphere, especially for the emission of biogenic VOC like isoprene and monoterpenes (Wu et al., 2020), ~~causingleading to~~ the variations of VOC species ~~whichthat~~ dominate  $k_{\text{NO}_3}$  towards VOC in different seasons.

~~The Previous works showed that the~~ VOC species which ~~dominantdominate~~ the  $\text{NO}_3$  reactivity vary greatly between different regions. In forests and rural areas, such as Pabstchum outside Berlin, Germany, the lush forests ~~emitemitted~~ a large ~~amountnumber~~ of monoterpenes and isoprene, accounting for the majority of  $k_{\text{NO}_3}$ , which ranged from 0.0025 to 0.01  $\text{s}^{-1}$  (~~Asaf et al., 2009~~);(~~Asaf et al., 2009~~). In semi-arid urban areas such as Jerusalem, the emissions of BVOC are less due to the sparser vegetation, and the maximum of  $\text{NO}_3$  reactivity was about 0.01  $\text{s}^{-1}$ . ~~Phenol, in which the phenol,~~ cresol and some monoolefins emitted by road traffic ~~arewere~~ the main contributors (~~Asaf et al., 2009~~)(Asaf et al., 2009). In ~~the~~ urban regions like Houston, ~~the~~ industrial emissions, including isoprene and other alkenes, dominated the  $\text{NO}_3$  reactivity (Stutz et al., 2010). In ~~the suburbs of the city's suburbs,~~ the  $k_{\text{NO}_3}$  may be jointly affected by anthropogenic and ~~biologicalbiogenic~~ volatile organic compounds. For example, the  $\text{NO}_3$  reactivity towards VOC in Xianghe, Beijing reached  $0.024 \pm 0.030 \text{ s}^{-1}$ , with ~~thea~~ maximum value of 0.3  $\text{s}^{-1}$  and minimum value of 0.0011  $\text{s}^{-1}$ . Isoprene, styrene, and 2-butene contributed to ~~the majoritymost~~ of the  $k_{\text{NO}_3}$  (Yang et al., 2020).

~~In addition to calculating  $k_{\text{NO}_3}$  by the measured VOC, an instrument was developed to directly measure  $k_{\text{NO}_3}$  in the atmosphere (Liebmann et al., 2017). On this basis, they presented the first direct measurement of  $\text{NO}_3$  reactivity in the Finnish boreal forest in 2017 and concluded that the  $\text{NO}_3$~~

带格式的: 字体: Times New Roman, 小四

reactivity was generally high with a maximum value of  $0.94\text{ s}^{-1}$ , displaying a strong diel variation with. The above  $\text{NO}_3$  reactivities are all calculated by the measurement of VOC concentrations. In addition to this method, an instrument was developed to measure  $k_{\text{NO}_3}$  in the atmosphere directly (Liebmann et al., 2017). They presented the first direct measurement of  $\text{NO}_3$  reactivity in the Finnish boreal forest in 2017. They concluded that the  $\text{NO}_3$  reactivity was generally high, with a maximum value of  $0.94\text{ s}^{-1}$ , displaying a strong diel variation with a nighttime mean value of  $0.11\text{ s}^{-1}$  and daytime value of  $0.04\text{ s}^{-1}$  (Liebmann et al., 2018a). In 2018, they presented the direct measurement in and above the boundary layer of a mountain site, with daytime values of up to  $0.3\text{ s}^{-1}$  and nighttime values close to  $0.005\text{ s}^{-1}$  (Liebmann et al., 2018b). Most importantly, the direct measurement revealed the existence of missing  $\text{NO}_3$  reactivity in ~~varies various~~ regions, which indicated the missing  $\text{NO}_3$  oxidation mechanisms, ~~and~~. These results largely improved the understanding of nighttime chemistry.

Nevertheless, the ~~field~~-direct ~~field~~ determination of  $k_{\text{NO}_3}$  is still extremely ~~lacked~~lacking, especially in urban regions: ~~at the current stage~~. Until now, most works about the VOC oxidation by  $\text{NO}_3$  ~~was were~~ usually based on short-term investigations, and the analysis of ~~the~~ nocturnal chemical process or reactivity was carried out based on the data of a few weeks or several months. ~~The studies~~Studies of nighttime chemistry based on long-term measurement data are ~~very~~ scarce (Vrekoussis et al., 2007; Wang et al., 2023; Zhu et al., 2022). The detailed VOC contributions to  $k_{\text{NO}_3}$ , and the relationship between certain VOC and total  $\text{NO}_3$  reactivity ~~in on~~ a long-time scale are ~~also~~ rarely studied. Our recent work reported that the increasing trend of ~~the~~  $\text{NO}_3$  production rate ~~is~~ caused by ~~the~~ anthropogenic emission changes, while the long-term and detailed  $\text{NO}_3$  loss budget is still uncertain to some extent (Wang et al., 2023). ~~(Wang et al., 2023)~~. Here, we attempt to look ~~for~~ insight ~~to into~~ the level, variations, and impacts of  $\text{NO}_3$  reactivity by using the one-year measurement of VOC in an urban site in Beijing, the role of unmeasured VOC species (monoterpenes) in the contributions of  $\text{NO}_3$  reactivity is also discussed. The long-term trend of  $\text{NO}_3$  reactivity is estimated by collecting the published VOC data and the ~~newly~~ proposed parameterization method. At last, ~~the regulation of  $\text{NO}_3$  oxidation of nocturnal VOC is oxidation by  $\text{NO}_3$  during~~ different seasons ~~is was~~ further evaluated.

## 2. Methods

### 2. Method

#### 2.1 Site description and instrumentation

The measurement was conducted at the campus of Peking University ( $39^\circ 99' \text{ N}$ ,  $116^\circ 30' \text{ E}$ ) ~~during~~ the whole year of 2019. The site is situated northeast of the Beijing city center and near two traffic roads, which ~~represents~~represent a typical urban and polluted area with fresh, anthropogenic emissions (Wang et al., 2017a). The measurements were made on a building roof with a height of 20 m above the ground. Measurements of VOC concentrations were performed using an automated gas chromatograph equipped with mass spectrometry or flame ionization detectors (GC-MS/FID). ~~There are 56 kinds of VOC are measured in total, in which monoterpenes are not valid. The volatile organic compounds were pretreated by pre-freezing and collected in the deactivated quartz empty capillary at extreme-low temperature ( $-150^\circ \text{ C}$ ), then heated and delivered into the analysis system. After separation by the double chromatographic column, the low-carbon compounds  $\text{C}_2\text{-C}_4$  were detected~~

带格式的: 字体: Calibri, 五号, 字体颜色: 自动设置

带格式的: List Paragraph1, 段落间距段前: 0 磅, 段后: 0 磅, 行距: 多倍行距 1.14 字行

by the FID detector, and the high-carbon compounds C<sub>5</sub>-C<sub>10</sub> were detected by the MS detector. There are 56 kinds of VOC measured in total (listed in Table S1 and the concentrations are depicted in Figure S1), in which monoterpenes measurement are not valid. NO<sub>x</sub> and O<sub>3</sub> were monitored by chemiluminescence (Thermo Scientific, 42i-TLE) and UV photometric methods (Thermo Scientific, 49i), respectively. A Tapered Element Oscillating Microbalance analyzer (TianHong, TH-2000Z1) was used to measure the mass concentration of PM<sub>2.5</sub>. The quality assurance and quality controls of data were implemented regularly (Chen et al., 2020). Photolysis frequencies were obtained by the Tropospheric Ultraviolet and Visible (TUV) model simulation. Hourly data were processed and used in the following analysis.

## 2.2 Estimation of monoterpenes

Since the measurement data did not include monoterpenes (~~MNTs~~MNT), we therefore use the measured isoprene and ~~modelled~~modeled concentration ratio of monoterpene to isoprene in the same region of the measurement site (named as Factor, Eq. 2) to estimate the ambient monoterpene concentrations (named as MNT<sub>obs</sub>, Eq. 3). The Factor was obtained by the regional model (WRF/CMAQ), more details of the model simulation setup can be found in Mao et al. (2022). Briefly, the regional model CMAQ (Community Multiscale Air Quality) version 5.2 was applied to simulate air quality in eastern China, with a horizontal resolution of 36 km. Specifically, the gas-phase mechanism of SAPRC-07 and aerosol module AERO6 were used. The meteorological fields were provided by Weather Research & Forecasting (WRF) Model version 4.2. The biogenic emissions were simulated by the MEGANv2.1, which was driven by WRF as well, and the emissions of open burning were estimated with FINN. The MEIC emission inventory for 2019 (obtained via private communication) was used to represent anthropogenic emissions over China, while the emissions in the areas outside China were provided by the REAS v3.2 inventory simulation.

$$Factor = \frac{[MNT_{sim}]}{[ISO_{sim}]} \quad \text{Eq. 2}$$

$$[MNT_{obs}] = [ISO_{obs}] \times Factor \quad \text{Eq. 3}$$

We used the Factor to estimate monoterpenes level rather than ~~modelled~~modeled monoterpene concentrations is due to the ~~modelled~~modeled isoprene is systematically higher than that of observation (Fig. S1), thus S2). Thus the using of the ~~modelled~~modeled Factor may be more reasonable. In Beijing, α-pinene and β-pinene were reported to have the highest abundance among monoterpenes (Cheng et al., 2018), with higher emissions in summer (Wang et al., 2018b; Xia and Xiao, 2019). Therefore, we use a weighted reaction rate coefficient approximated by the averagedaverage value of α-pinene and β-pinene reaction rate coefficients with NO<sub>3</sub> in the following calculations. Since the emissions of sesquiterpenes in BVOC are much lower than that of isoprene, monoterpenes, and other BVOC, thus we didn'tdid not consider NO<sub>3</sub> reactivity towards the contribution of sesquiterpenes to the reactivity. The detailed average diurnal variations of Factor are listed in Table S2.

$$Factor = \frac{[MNT_{sim}]}{[ISO_{sim}]} \quad \text{Eq. 2}$$

$$[MNT_{obs}] = [ISO_{obs}] \times Factor \quad \text{Eq. 3}$$

- 带格式的：字体：非倾斜，非上标/下标
- 带格式的：下划线颜色：自动设置
- 带格式的：非上标/下标
- 带格式的：下划线颜色：自动设置
- 带格式的：fontstyle01，字体：小四
- 带格式的：fontstyle01
- 带格式的：下划线颜色：自动设置
- 带格式的：字体：五号，字体颜色：红色

### 2.3 VOC oxidation rate by NO<sub>3</sub>

To study the reaction of NO<sub>3</sub> and VOC during the nighttime, we estimated the NO<sub>3</sub> concentrations by steady-state calculation. This method is widely used to estimate the concentrations of short-lived substances ~~like NO<sub>3</sub>, by~~ assuming its production and loss rates are balanced in a specific time range. Given sufficient time, the steady state can be reached for NO<sub>3</sub> at night, in which the production and loss terms are approximately balanced (Brown, 2003; Crowley et al., 2010). ~~The~~ Here the production terms of NO<sub>3</sub> ~~is~~ are the reaction of NO<sub>2</sub> and O<sub>3</sub>, and the loss terms of NO<sub>3</sub> ~~includes~~ include reactions with VOC, reaction with NO, heterogeneous reaction, and photolysis. The steady-state NO<sub>3</sub> mixing ratios are expressed by Eq. 4 (Brown and Stutz, 2012).

$$[NO_3]_{ss} = \frac{k_{NO_2+O_3}[NO_2][O_3]}{\sum k_i \times [VOC_i] + k_{NO+NO_3}[NO] + J_{NO_3} + k_{het}K_{eq}[NO_2]} \quad \text{Eq. 4}$$

Where  $J_{NO_3}$  is the sum of the photolysis coefficients of the two photolysis reactions of NO<sub>3</sub>. The  $k_{het}$  is the heterogeneous uptake rate of N<sub>2</sub>O<sub>5</sub> on the aerosol surface, which can be calculated by Eq. 5.

$$k_{het} = 0.25 \times \gamma \times S_a \times c \quad \text{Eq. 5}$$

Where  $\gamma$  is the dimensionless uptake coefficient of N<sub>2</sub>O<sub>5</sub> parameterized by Eq. 6 (Evans and Jacob, 2005; Hallquist et al., 2003; Kane et al., 2001),  $S_a$  (m<sup>2</sup> m<sup>-3</sup>) is the aerosol surface area density estimated by the level of PM<sub>2.5</sub> (Wang et al., 2021), and  $c$  is the mean molecular velocity of N<sub>2</sub>O<sub>5</sub>.

$$\gamma = \alpha \times 10^\beta$$

$$\alpha = 2.79 \times 10^{-4} + 1.3 \times 10^{-4} \times RH - 3.43 \times 10^{-6} \times RH^2 + 7.52 \times 10^{-8} \times RH^3$$

$$\beta = 4 \times 10^{-2} \times (T - 294) \quad (T > 282K)$$

$$\beta = -0.48 \quad (T < 282K) \quad \text{Eq. 6}$$

The reaction rate coefficients of NO<sub>2</sub> and O<sub>3</sub>, NO and NO<sub>3</sub>, and the equilibrium constant for the forward and reverse Reactions (R4) and (R5) are temperature dependent. We have adopted JPL evaluation reports for the reaction rate coefficients. The time series of hourly-related parameters in estimating the steady-state NO<sub>3</sub> and the diurnal cycle of NO<sub>3</sub> concentrations were shown in Fig. S2S3 and Fig. S3S4. To compare the VOC oxidation ~~of~~ by NO<sub>3</sub> ~~towards~~ VOC with other oxidants, we estimated OH concentrations by the slope ~~that~~ extracted from the measured OH and  $J_{O^1D}$  (s<sup>-1</sup>) in North China (Tan et al., 2017)) (Eq. 7), where  $J_{O^1D}$  used in this study was obtained by the TUV model simulations. The VOC oxidation rate ( $R_{NO_3}$ ) and the ratio of VOC oxidized by NO<sub>3</sub> to the total oxidation rate can be calculated by Eq. 8.

$$[OH] = 4.1 \times 10^{11} \text{ cm}^{-3} \text{ s}^{-1} \times J_{O^1D} \quad \text{Eq. 7}$$

$$R_{NO_3} \approx \frac{\sum k_i \times [VOC_i][NO_3]}{\sum k_i \times [VOC_i][OH] + \sum k_i \times [VOC_i][NO_3] + \sum k_i \times [VOC_i][O_3]} \quad \text{Eq. 8}$$

where  $k_i$  represents the corresponding reaction rate coefficients of different VOC with oxidants.

### 3. Results and discussion

#### 3.1 NO<sub>3</sub> reactivity calculated by measured VOC

During the campaign, the hourly  $k_{\text{NO}_3}$  towards measured VOC (named as  $k_{\text{NO}_3\_mea}$ ) highly varied from  $<10^{-4}$  to  $0.083 \text{ s}^{-1}$  with campaign-averaged value ( $\pm$  standard deviation) of  $0.0032 \pm 0.0042 \text{ s}^{-1}$ . The  $k_{\text{NO}_3\_mea}$  displayed a strong diel variation on the annual average (Fig. S4S5). In previous studies, the NO<sub>3</sub> reactivity towards VOC was reported to be  $0.024 \pm 0.030 \text{ s}^{-1}$  on average in a suburban site in summer in North China (Yang et al., 2020); and highly varied between  $0.005 - 0.3 \text{ s}^{-1}$  in the mountaintop site in summer (Liebmann et al., 2018c). Our result is one order of magnitude lower, which may reflect the huge difference of  $k_{\text{NO}_3\_mea}$  in different environments and sampling time. Certainly, it may be attributed to the reason that calculated  $k_{\text{NO}_3}$  here did not include some species, such as monoterpenes, phenol, cresol and so on. The diurnal variations of  $k_{\text{NO}_3\_mea}$  had strong seasonal variability (Fig. S5S6). The diurnal variations in winter and spring were relatively weak, and the variations in summer and autumn were largest, with clear peaks at 9:00-10:00 and 15:00, respectively. The  $k_{\text{NO}_3\_mea}$  in spring, summer, and autumn reached the daily maximum value between 8:00 a.m. and 10:00 a.m. (spring:  $0.0034 \text{ s}^{-1}$ , summer:  $0.0083 \text{ s}^{-1}$ , autumn:  $0.0057 \text{ s}^{-1}$ ). In winter, it reached the maximum value of  $0.0033 \text{ s}^{-1}$  at about 22:00.

As shown in Fig. 1a, the  $k_{\text{NO}_3\_mea}$  reached the highest in August and lowest in February, which was largely affected by the level of isoprene and styrene. For example, isoprene contributed ~80% to the reactivity in August. The  $k_{\text{NO}_3\_mea}$  towards isoprene reached the maximum in August and the minimum in February, which was consistent with the previously reported change in isoprene concentrations in Beijing (Cheng et al., 2018). Figure 1b The  $k_{\text{NO}_3\_mea}$  shows a large seasonal difference in  $k_{\text{NO}_3\_mea}$  with the average value of  $0.0024 \pm 0.0026 \text{ s}^{-1}$ ,  $0.0067 \pm 0.0066 \text{ s}^{-1}$ ,  $0.0042 \pm 0.0037 \text{ s}^{-1}$ ,  $0.0027 \pm 0.0028 \text{ s}^{-1}$  from spring to winter. Table S2S3 shows the specific contributions of the top six species to  $k_{\text{NO}_3\_mea}$  in different seasons (and Fig. S4). Isoprene was the dominant species, accounting for 40.0%, 77.2%, and 43.2% in spring, summer, and autumn. By comparison, styrene only played a leading role in winter, accounting for 39.8%. Among the species which contributed to  $k_{\text{NO}_3\_mea}$  in Beijing, isoprene and styrene contributed most to the overall  $k_{\text{NO}_3\_mea}$  (60%~90%), followed by cis-2-butene, trans-2-butene, trans-2-pentene, and propylene (5%~15%) with another individual VOC less than 2%. Our results are consistent with previous studies in Beijing that  $k_{\text{NO}_3}$  was mainly contributed by isoprene (Yang et al., 2020), indicating the critical role of isoprene in NO<sub>3</sub> reactivity in Beijing. From summer to autumn, the dominant species changed from isoprene to styrene, while from winter to spring, the dominant species changed from styrene to isoprene. This indicated the AVOC and BVOC controls control  $k_{\text{NO}_3\_mea}$  alternately. Overall, the  $k_{\text{NO}_3\_mea}$  displayed a characteristic of high in summer and autumn and low in winter and spring.

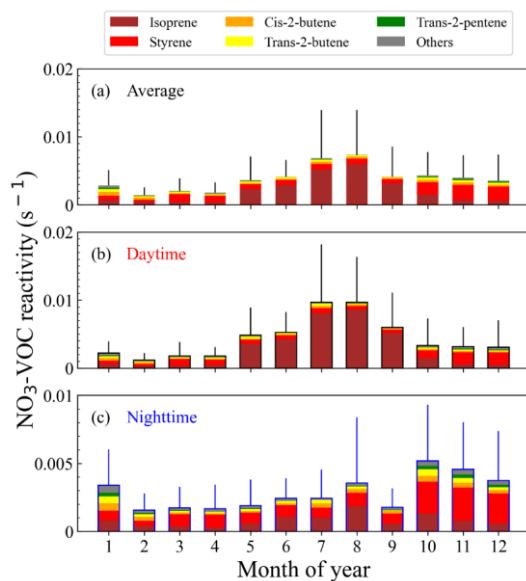
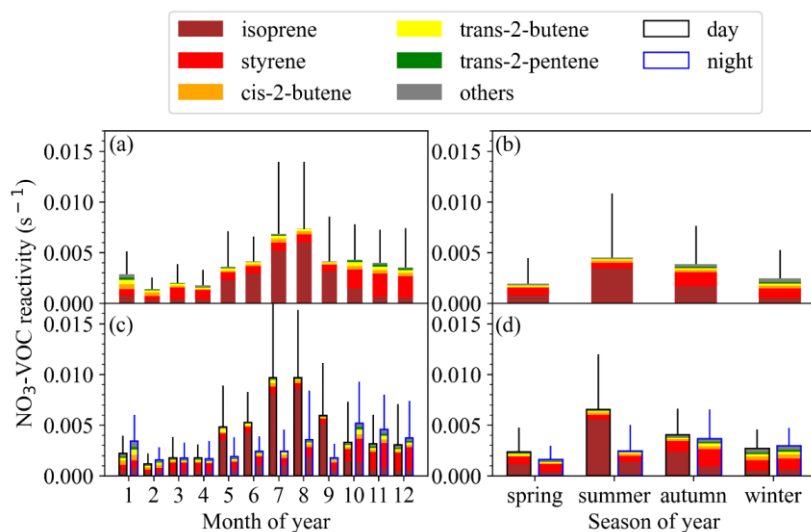


**Figure 1.** (a-b) Histograms of monthly and seasonal averaged  $\text{NO}_3$ -VOC reactivity and the compositions. (c-d) Histograms of monthly and seasonal averaged  $\text{NO}_3$ -VOC reactivity and the compositions divided into day (a), daytime (black frames) (b), and nighttime (blue frames) (c). The color denotes the contributions of different VOC species. The black and blue lines represent the error bars of the reactivity ( $\pm$  standard deviation).

带格式的：默认段落字体，字体：Calibri，五号，非倾斜，字体颜色：自动设置

带格式的：默认段落字体，字体：Calibri，五号，字体颜色：自动设置



deviations).

Figure 1b-c shows the  $k_{\text{NO}_3\text{_{mea}}}$  towards measured VOC display clear day-night differences in summer and winter, especially in summer. The  $\text{NO}_3$  reactivity towards VOC in the daytime reached the value of  $0.010\text{ s}^{-1}$  in July and August, which was much higher than  $0.002\text{ s}^{-1}$  in the nighttime. The variations were mainly caused by the diel variations of isoprene concentrations. Reversely, the reactivity was higher at night and lower in the daytime in winter, which was due to the high AVOC level in the morning and at night (Lee and Wang, 2006). Specifically, styrene concentrations at night increased significantly in the stable nocturnal boundary layer, resulting in relatively higher reactivity.

In urban areas of Beijing, isoprene origins from anthropogenic and ~~biological~~biogenic sources, in which the anthropogenic sources of isoprene are mainly traffic emissions (Li et al., 2013; Riba et al., 1987; Zou et al., 2015). ~~In summer, isoprene mainly origins from plant, and in winter origins from the combustion of engine fuel. In spring and autumn, there are mixed effects of anthropogenic and biological origins (Li et al., 2013). The isoprene emissions of biological~~The isoprene emissions from biogenic sources in Beijing were one order of magnitude larger than that of anthropogenic sources (Yuan et al., 2009). This indicates the concentrations of isoprene at the environmental level in the urban areas of Beijing ~~isare~~ not affected by the traffic vehicles, but mainly by plants ~~in Beijing~~ (Cheng et al., 2018). As an aromatic hydrocarbon, styrene origins from both anthropogenic and biogenic sources in the atmosphere (Miller et al., 1994; Mogel et al., 2011; Schaeffer et al., 1996; Tang et al., 2000; Zielinska et al., 1996; Zilli et al., 2001), such as the laminar flame of engine fuel (Meng et al., 2016), industrial production (Radica et al., 2021) and other human activities. The dominant source of styrene in Beijing is the local ~~vehiclesvehicle~~ emissions (Li et al., 2014). Some vegetation, such as evergreen and oleander, can ~~also~~ release natural styrene (Wu et al., 2014), however, due to the dense industrial distribution in the urban area and the much lower level of these biogenic styrene compared with isoprene, we ~~believedbelieve~~ that the styrene in the atmosphere in Beijing is mainly resulted from anthropogenic origins. It is believed that human activities in winter, such as heating, gasoline, and diesel combustion, increased, meanwhile, the reduction of temperature and radiation resulted in the reduction of biogenic isoprene emissions, explained the conversion of dominance of  $\text{NO}_3$  reactivity from summer to winter.

The  $\text{NO}_3$  reactivity towards MNTs (named as  $k_{\text{NO}_3\text{_{MNTs}}}$ ) was estimated by the method mentioned in section 2.2. After taking MNTs into account, the total  $k_{\text{NO}_3}$  (named as  $k_{\text{NO}_3\text{_{total}}}$ ) was greatly enlarged, with the campaign-averaged value of  $0.0061 \pm 0.0088\text{ s}^{-1}$ , resulting in our results comparable with previous research results. The  $\text{NO}_3$  reactivity towards MNTs was higher in autumn and winter and lower in spring and summer (Fig. S7). Considering the corresponding reactivity towards monoterpenes, the total  $\text{NO}_3$  reactivity towards VOC changed from (summer > autumn > winter > spring) to (autumn > winter > summer > spring), highlighting the impact of the monoterpene variations on the reactivity. The  $\text{NO}_3$  reactivity towards MNTs displayed significant differences between daytime and nighttime (Fig. S7c-d). The reactivity at night in all months was higher than that in the daytime, especially from October to January, highlighting the role of biogenic monoterpenes in nocturnal  $\text{NO}_3$  chemistry (Li et al., 2013; Riba et al., 1987). To evaluate the contribution of monoterpenes to the total  $k_{\text{NO}_3}$ , we calculated the fraction ( $F_{\text{MNTs}}$ ) by Eq. 9.

域代码已更改

$$F_{MNTs} = \frac{k_{NO_3, MNTs}}{k_{NO_3, total}} \quad \text{Eq. 9}$$

Figure 2a displays the differences between the  $k_{NO_3, mea}$  and  $k_{NO_3, total}$ . Monoterpenes were very important for  $NO_3$  reactivity, and the  $F_{MNTs}$  varied from 40% to 80%, with strong seasonal variations. The MNTs accounted for  $NO_3$  reactivity of nearly 80% in winter and spring. In the seasons when isoprene no longer dominated, the measured reactivity accounted for a small fraction, and the corresponding reactivity towards AVOC, such as styrene, was smaller than that of monoterpenes. As shown in Fig. 2b, the measured VOC had high fractions in the daytime and low at night, especially in May and August. The measured VOC in the daytime accounted for more than 60% of  $k_{NO_3, total}$ , which was closely related to the increasing concentrations of isoprene in the summer daytime. The reactivity towards MNTs accounted for a large fraction of reactivity at night.

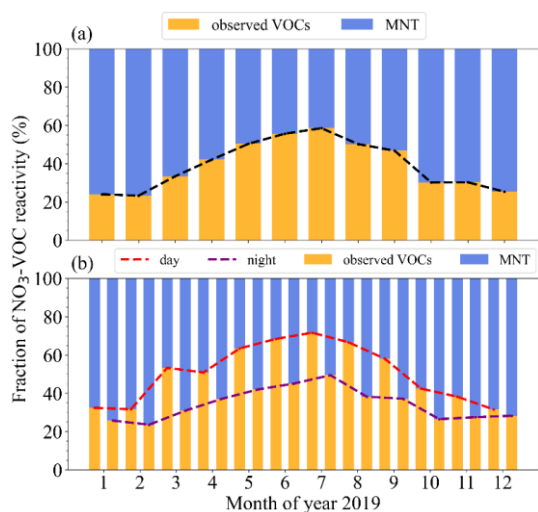


**Figure 2.** (a) Fractions of the  $k_{NO_3, total}$ . (b) Fractions of the  $k_{NO_3, total}$  divided into daytime (left) and nighttime (right). The colors on the stacked bar plot indicate the different fractions as they are donated in the legend. The lines represent the monthly-averaged variations of the  $NO_3$  reactivity towards MNTs.

### 3.2 Parameterization of $NO_3$ reactivity

We examined the correlation of key VOC concentrations and  $k_{NO_3, mea}$ . Figure-S6, S8 gives the case in January, for example. To a certain extent, the variations of  $k_{NO_3, mea}$  were closely linked to the variations of the concentrations of main contributors. It is worth noting that in January, trans-2-butene had a higher correlation coefficient with  $k_{NO_3, mea}$ , which exceeded that of isoprene and styrene. This indicates that higher contributions may not imply a stronger correlation. Fig. 23 shows the correlation coefficients and the fitting equations between VOC concentrations and  $k_{NO_3}$  in each month (detailed in Table S3S4). According to the correlation coefficients, we can select the strongest indicator corresponding to the certain month as the variable of the parameterization method. Here we didn't

import the VOC with small contributions into the parameterization method, because these indicators had no practical significance for  $k_{\text{NO}_3\_mea}$ . In this way, we established the first parameterization method (Method 1) by using the strongest indicator in each month and which can be found in Table S3S4 (Eq. 10):

$$NO_3 \text{ reactivity}_{sim1} = a_i \times [VOC_i] + b_i \quad \text{Eq. 10}$$

where,  $a_i$ ,  $b_i$ , and  $[VOC_i]$  respectively represent the slope, the intercept, and the VOC species concentrations (ppbv) used for parameterization in each month. Throughout the year, the correlation coefficients between isoprene concentrations and  $k_{\text{NO}_3\_mea}$  were high throughout the year, ranging from 0.67 to 0.98, especially in summer. The correlation coefficients between styrene concentrations and the reactivity reached a maximum in autumn and winter, which can clearly display the indication of these two species (isoprene and styrene) in different seasons.

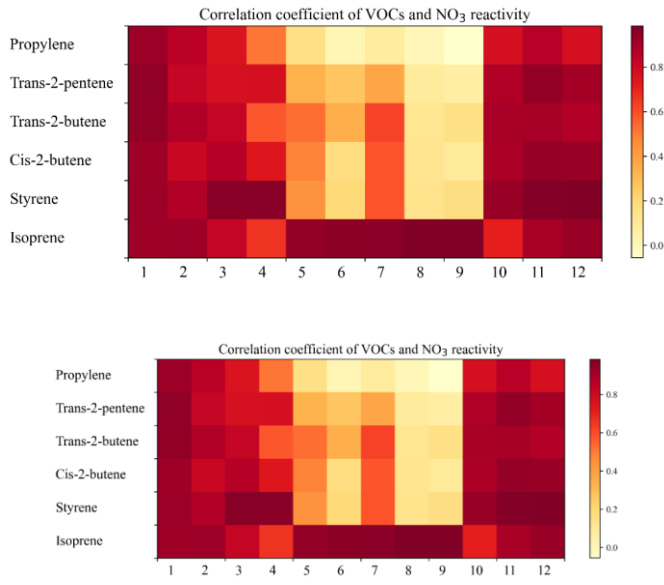


**Figure 23.** The thermodynamic diagram of the monthly correlation between VOC concentrations and  $k_{\text{NO}_3\_mea}$ . Colored blocks indicate different correlations, by which the best indicator can be selected for the parameterization method of each month.

Besides the indicator parameterization method, we can also select only a part of VOC that contribute most of  $k_{\text{NO}_3\_mea}$  as a representative. Here we approximated  $\text{NO}_3$  reactivity towards total VOC to the reactivity towards these top 6 species, namely: isoprene, styrene, cis-2-butene, trans-2-butene, trans-2-pentene, and propylene. Thus, the second parameterization method (Method 2) can be expressed by Eq. 11:

带格式的：默认段落字体，字体：Calibri，五号，非倾斜，字体颜色：自动设置

$$NO_3 \text{ reactivity}_{sim2} = \sum_{i=1}^6 k_i \times [VOC_i] \quad \text{Eq. 11}$$

where  $[VOC_i]$  is the VOC concentrations and  $k_i$  is the corresponding reaction rate coefficients with  $NO_3$ . It should be noted that this parameterization method of  $NO_3$  reactivity towards VOC may be localized.

To evaluate the effectiveness of the two parameterization methods established above, we estimated the  $k_{NO_3}$  in the different time ~~scales~~, and compared them with the determined  $k_{NO_3\_mea}$  by all measured VOC. As shown in Fig. S7S9, both ~~two~~ methods can well capture the level and variations of  $k_{NO_3\_mea}$ , indicating the parametrization feasibility. Method 1 can easily and quickly estimate  $NO_3$  reactivity towards VOC ~~by~~ using a single indicator. In areas where a single VOC specie dominates,  $NO_3$  reactivity towards VOC ~~is dominated by a single VOC specie~~ for a long time, such as forest areas, suburbs, and rural areas (BVOC dominant), this method would have a good performance. Method 2 had a better performance, while more VOC species are needed. In urban areas, especially in urban areas where the contributors had different chemo diversity with strong seasonality, this method should be more suitable. Since the two methods lower the bar for estimating  $NO_3$  reactivity by using VOC measurement data, we can look into investigate the level of  $NO_3$  reactivity ~~by~~ using the reported VOC measurement data in the past.

We collected the historical measurement data of VOC concentrations in Beijing (Supporting file. S1) and estimated  $NO_3$  reactivity ~~by the using~~ parameterization methods. We found the level of  $NO_3$  reactivity mainly ranged from 0.001 to 0.1  $s^{-1}$  in Beijing in the past decades (Fig. 3). ~~Due to the limitation of data, we cannot find a trend of  $NO_3$  reactivity before 2011. While during 2011-2020,4).~~ During 2014-2020, a large amount of VOC data in urban Beijing presented and be collected in this study. We calculated the  $k_{NO_3\_mea}$  by detailed VOC ~~with respect to concerning~~ the data provided by the ~~literatures literature~~, and estimated the  $NO_3$  reactivity by parameterization methods if the reported data in the literatures ~~is are~~ limited. As shown in Fig. 3, ~~an overall decrease trend of 4,~~  $NO_3$  reactivity ~~can be found during 2011-2020 was relatively lower after 2014 than before.~~ We inferred that the level of isoprene during this period may be varied small; since the change of biogenic emission ~~unlikely to change much may not be significant~~. Thus, we proposed that the ~~decrease of lower~~  $NO_3$  reactivity during the past decade may be attributed to the anthropogenic emission reduction of anthropogenic VOC. It should be noted that this estimation suffers from ~~the~~ uncertainty, nevertheless, this trend and characterization of  $NO_3$  reactivity in Beijing is helpful to understand the nighttime chemistry in Beijing.

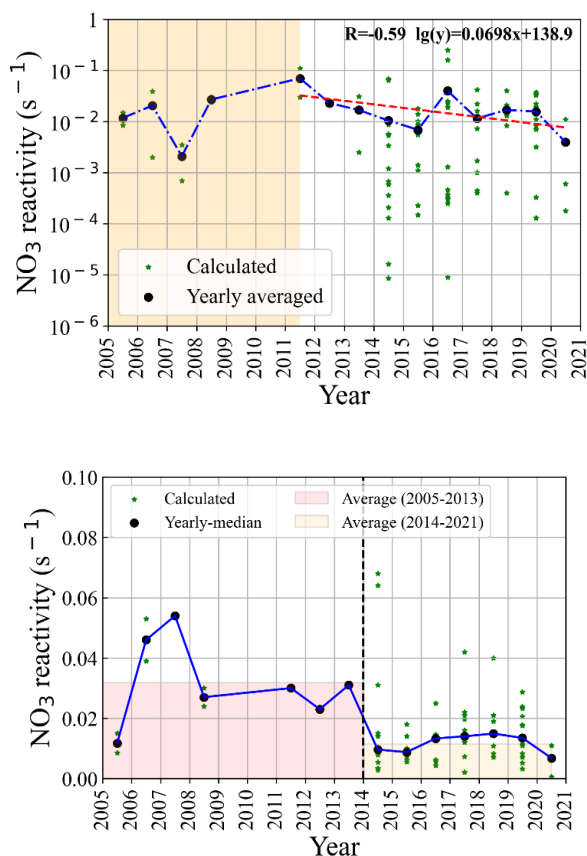


**Figure 34.** The reconstructed NO<sub>3</sub> reactivity calculated by the reported VOC concentrations in Beijing calculated the reconstructed NO<sub>3</sub> reactivity record from 2005-2021. The averaged NO<sub>3</sub> reactivity calculated by the reported VOC data in each campaign is plotted as the star. The yearly averaged median values of NO<sub>3</sub> reactivity (black dot) between 2011-2019 shows a decline in each year show high during 2005-2013 and relatively low during 2014-2021. It should be noted that the monoterpenes are not considered here.

### 3.3 NO<sub>3</sub> reactivity towards monoterpenes

After taking MNTs into account, the total  $k_{\text{NO}_3}$  (named as  $k_{\text{NO}_3\text{-total}}$ ) was greatly enlarged, with campaign averaged value of  $0.0061 \pm 0.0088 \text{ s}^{-1}$ , resulting in our results comparable with previous research results. The NO<sub>3</sub> reactivity towards MNTs (named as  $k_{\text{NO}_3\text{-MNTs}}$ ) was higher in autumn and winter and lower in spring and summer (Fig. S8). Considering the corresponding reactivity towards monoterpenes, the total NO<sub>3</sub> reactivity towards VOC changed from (summer > autumn > winter > spring) to (autumn > winter > summer > spring), highlights the impact of the monoterpene variations

on the reactivity. The  $\text{NO}_2$  reactivity towards MNTs displayed significant differences between daytime and nighttime (Fig. S8e-d). The reactivity at night in all months was higher than that in the daytime, especially from October to January, highlights the role of biogenic monoterpenes in nocturnal  $\text{NO}_2$  chemistry (Li et al., 2013; Riba et al., 1987). To compare the measured and the total  $\text{NO}_2$  reactivity towards VOC, we calculated the fraction ( $F_{\text{MNTs}}$ ) by Eq. 12:

$$F_{\text{MNTs}} = \frac{k_{\text{NO}_2\text{-MNTs}}}{k_{\text{NO}_2\text{-total}}} \quad \text{Eq. 12}$$

Figure 4a displays the differences between the  $k_{\text{NO}_2\text{-mea}}$  and  $k_{\text{NO}_2\text{-total}}$ . Monoterpenes were very important for  $\text{NO}_2$  reactivity, and the  $F_{\text{MNTs}}$  varied from 40% to 80%, with strong seasonal variations. The MNTs accounted for  $\text{NO}_2$  reactivity nearly 80% in winter and spring. In the seasons when isoprene no longer dominated, the measured reactivity accounted for a small fraction, and the corresponding reactivity towards AVOC such as styrene was smaller than that of monoterpenes. As shown in Fig. 4b, the measured VOC had high fractions in the daytime and low at night. Especially in May and August. The measured VOC in the daytime accounted for more than 60% of  $k_{\text{NO}_2\text{-total}}$ , which was closely related to the increasing concentrations of isoprene in the summer daytime. The reactivity towards MNTs accounted for a large fraction of reactivity at night.

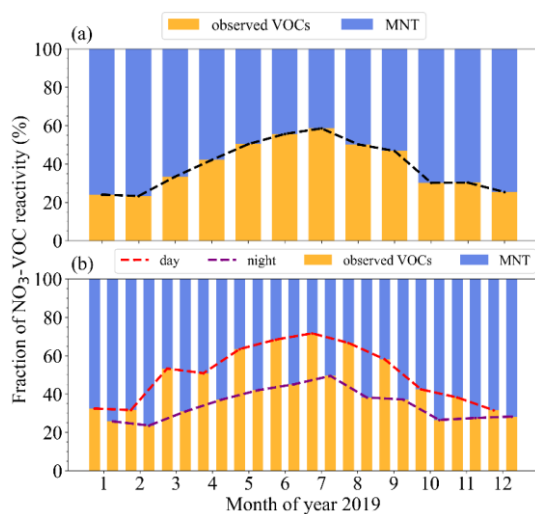


**Figure 4.** (a) Fractions of the  $k_{\text{NO}_2\text{-total}}$ . (b) Fractions of the  $k_{\text{NO}_2\text{-total}}$  divided into daytime (left) and nighttime (right). The colors on the stacked bar plot indicate the different fractions as they are donated in the legend. The lines represent the monthly-averaged variations of the  $\text{NO}_2$  reactivity towards MNTs.

After considering MNTs, we updated the parameterization method established before by using the relationship between reactivity and VOC concentrations, including monoterpenes. The updated parameterization Method 1 used the same principle as introduced in Sect 3.2, with fitting slopes changing significantly (Fig. S9Figure. S10). Table S4 gives S5 shows the specific correlation

域代码已更改

coefficients between six key VOC concentrations and  $k_{\text{NO}_3\text{ total}}$ . The updated Method 2 considered the sum contributions of six VOC and the estimated MNTs by isoprene concentration. We reevaluated the two updated parameterization methods (single VOC and six VOC, respectively). Overall, the performance of the two methods are reasonable, and the updated Method 1 is better than that of Method 2 in general (Fig. S10, S11). We evaluated this parameterization on datasets of other years (shown in Fig S12) and showed a robust performance.

### 3.4.3 Nighttime VOC oxidation

Here we examined the role of  $\text{NO}_3$  in the VOC oxidation in Beijing 2019. As shown in Fig. S13, OH oxidized most of VOC during the daytime, with the oxidation rate reaching the maximum value of  $0.6 \text{ pptv s}^{-1}$  in the afternoon. Compared with OH, the VOC oxidation rates by  $\text{O}_3$  and  $\text{NO}_3$  in the daytime were remarkably lower. From 18:00 to 6:00, the characteristics of nocturnal chemical in Beijing were significant. The ratios of VOC oxidized by  $\text{NO}_3$  kept above 80%, and the contribution of  $\text{O}_3$  was relatively weak, which is consistent with that reported in high  $\text{NO}_x$  regions (Chen et al., 2019; Edwards et al., 2017; Wang et al., 2018a). The VOC oxidation rate by  $\text{NO}_3$  presented a single peak at 19:00 with the value of  $0.25 \text{ pptv s}^{-1}$ , which is the same magnitude as that by OH in the daytime, illustrating the importance of  $\text{NO}_3$  in VOC oxidation as shown in the previous studies (Wang et al., 2017a), highlighting the importance of nocturnal chemistry for organic nitrate and SOA formation.

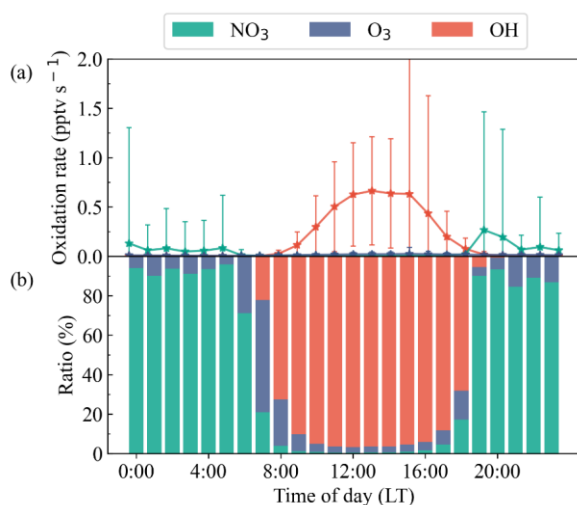


**Figure 5.** (a) Median diurnal profile of VOC oxidation rate by OH,  $\text{NO}_3$  and  $\text{O}_3$ . The colored lines are error bars (+standard deviation). (b) Fractions of VOC oxidation rate by atmospheric oxidants.

The VOC oxidation rate by  $\text{NO}_3$  and oxidation fractions had strong seasonal variabilities in Beijing. As shown in Fig. S14, the nighttime oxidation rate (summer > spring > autumn > winter) was affected by  $\text{NO}_3$  concentrations and the total  $\text{NO}_3$  reactivity towards VOC. In summer, the  $\text{NO}_3$  oxidation rate

presented a single peak, with a maximum value of 0.7 pptv s<sup>-1</sup> at 20:00, and remained around 0.1 pptv s<sup>-1</sup> at the rest of the night. The rate at 21:00-5:00 was relatively constant. The rate in winter was lower, with the two maximum values of 0.06 pptv s<sup>-1</sup> presented at 19:00 and 4:00, which were further lower than the average value of the other three seasons. The results were good agreement with the previous studies, in which the VOC oxidation rate by NO<sub>3</sub> concentrations contained was high from 19:00-23:00 (Wang et al., 2017b). There was a competition between NO<sub>3</sub> and O<sub>3</sub> in the nighttime VOC oxidation in Beijing. Although the NO<sub>3</sub> oxidation rate at night was higher than that of O<sub>3</sub> throughout the year, the changes of O<sub>3</sub> oxidation rate had a significant impact on significantly impacted the ratios of VOC oxidized by NO<sub>3</sub>. The ratios of nighttime VOC oxidized by NO<sub>3</sub> in Beijing were higher in autumn, and then in spring, summer, and winter. Although the O<sub>3</sub> concentrations in winter decreased, the competitiveness of NO<sub>3</sub> in VOC oxidation decreased more due to the decline of NO<sub>3</sub> concentrations. The competitiveness of O<sub>3</sub> in VOC oxidation was relatively enhanced, resulting in a significant decline in the ratios of VOC oxidized by NO<sub>3</sub>.

### 3.5 Regulation of nighttime VOC oxidation

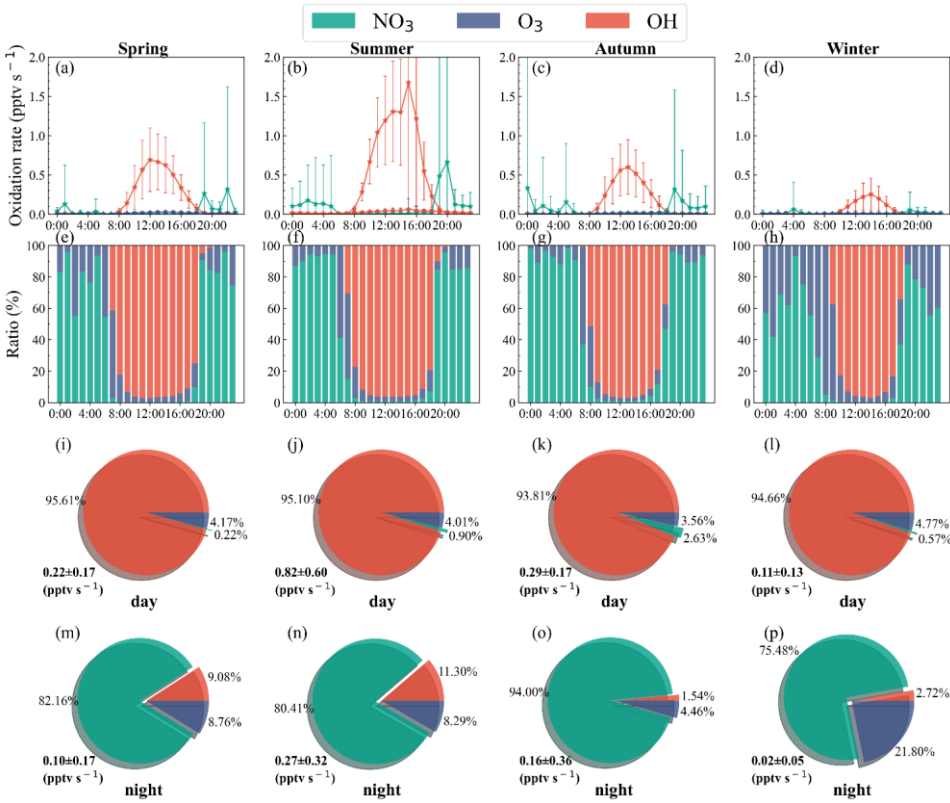


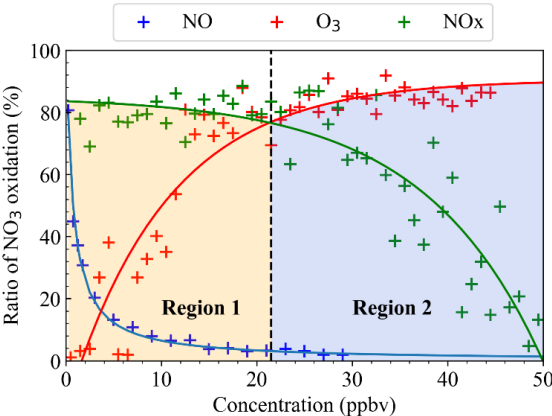
Figure 5. (a-d) Median diurnal profiles ( $\pm$ standard deviation) of VOC oxidation rate by atmospheric



oxidants in different seasons. (e-h) Fractions of VOC oxidation rate by atmospheric oxidants in different seasons. (i-p) Pie charts representing the daytime and the nighttime VOC oxidation rate by OH, NO<sub>3</sub>, and O<sub>3</sub> during different seasons, with the averaged values and standard deviations.

### 3.4 Relationship between O<sub>3</sub>/NO<sub>x</sub> and nocturnal VOC oxidation by NO<sub>3</sub>

To understand the importance of nighttime VOC oxidized by NO<sub>3</sub>, we defined the fraction of VOC oxidation rate by NO<sub>3</sub> to the total oxidation rate as nocturnal VOC oxidation ratio by NO<sub>3</sub> ( $R_{NO_3}$ , see Section 2.3 for its calculation) and explored the relationship between the nocturnal oxidation ratios of NO<sub>3</sub> ( $R_{NO_3}$ ) ratio and the nighttime concentrations of NO, O<sub>3</sub> and NO<sub>x</sub>/NO<sub>x</sub>. It is found that a strong nonlinear relationship between them (shown in Figure 6). The  $R_{NO_3}$  had negative correlation coefficients with NO concentrations. With the increase of NO concentrations at night, the ratios decreased exponentially. When the NO concentrations increased at low NO condition, it could cause a significant decline in the ratios of VOC oxidized by NO<sub>3</sub>. While at high NO condition, the ratios were not sensitive to the increase of NO concentrations (Fig. S42S14), indicating that the nighttime NO concentrations in Beijing strongly controlled the ratios effectively. It can be expected since the increase of NO concentrations controlled the NO<sub>3</sub> loss term, then caused the decrease of NO<sub>3</sub> concentration. When the NO concentrations exceeded a threshold value, (7 ppbv), the NO<sub>3</sub> loss was totally dominated by NO.



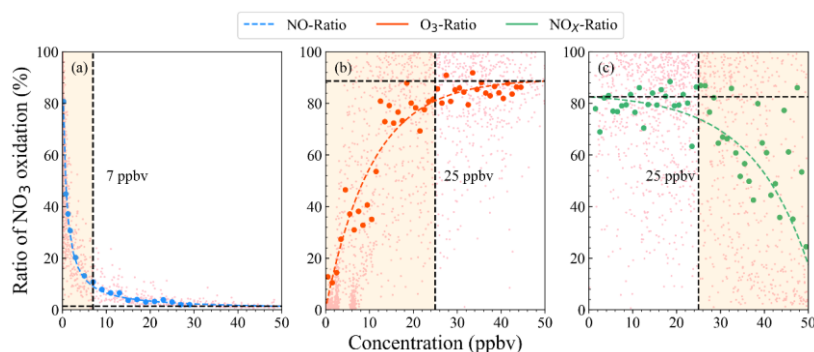


**Figure 6.** Fitting diagrams between the ratios of nighttime VOC oxidized by  $\text{NO}_3$  and the concentrations of  $\text{NO}$ ,  $\text{O}_3$  and  $\text{NO}_x$ . In Region 1, the ratio is more sensitive to  $\text{O}_3$ , while less sensitive to  $\text{NO}_x$ . In Region 2, it is more sensitive to  $\text{NO}_x$ , while less sensitive to  $\text{O}_3$ : (a),  $\text{O}_3$  (b), and  $\text{NO}_x$  (c). The light pink scattered dots represent the oxidation ratios at different concentrations, and the solid dots represent the median value of each bin of oxidation ratios corresponding to each concentration range. Colored dot lines represent the fitting results of the solid median dots. And the black dot line in each panel shows a threshold to divide the curve into two regimes. In (a), the regime is divided into  $\text{NO}$ -limited ( $<7$  ppbv) and  $\text{NO}$ -saturated ( $>7$  ppbv); in (b) and (c), a threshold of 25 ppbv divide the curves into  $\text{NO}_x$  ( $\text{O}_3$ ) limited and saturated regimes. The results showed in (b) and (c) are representative of low  $\text{NO}$  condition ( $<7$  ppbv).

The ratios of nighttime VOC oxidized by  $\text{NO}_3$  also had a strong nonlinear relationship with  $\text{O}_3$  and  $\text{NO}_x$  concentrations.  $\text{O}_3$  concentrations have one positive and one negative contribution to the  $R_{\text{NO}_3}$ . The positive effect is that increasing  $\text{O}_3$  concentration ~~increase~~ increases the  $\text{NO}_3$  production rate, which ~~increase~~ increases the  $\text{NO}_3$  steady-state concentrations and then increase the ratios. And the negative is increasing  $\text{O}_3$  concentrations ~~increase~~ increases the reaction rate between VOC and  $\text{O}_3$ , which increase the competitiveness of  $\text{O}_3$  in VOC oxidation and then decrease the ratios. Figure S12S14 also shows the relationship between the  $R_{\text{NO}_3}$  and the concentrations of  $\text{O}_3$ . While  $\text{O}_3$  concentrations were below 21.525 ppbv, the ratios were very sensitive to  $\text{O}_3$  level, which fast increased with  $\text{O}_3$  concentrations. While the ratio ~~become~~ became not sensitive and remained relatively constant when the  $\text{O}_3$  concentrations exceeded 21.525 ppbv. It can be explained that when the  $\text{O}_3$  concentrations were low, the  $\text{NO}_3$  production rate was more sensitive to the increase of  $\text{O}_3$  concentrations. In this case,  $\text{O}_3$  mainly affects the ratios positively. When the  $\text{O}_3$  concentrations were high, the positive effect of  $\text{O}_3$  tended to be constant, ~~indicates~~ indicating the two opposite effects ~~overall keep~~ kept in balance.

When the  $\text{NO}_x/\text{NO}_x$  concentrations were low (i.e.,  $<21.5$ ,  $<25$  ppbv), the  $R_{\text{NO}_3}$  ~~werewas~~ less sensitive to  $\text{NO}_x/\text{NO}_x$ , remaining relatively constant with the further increase. It is believed that the increase of  $\text{NO}_3$  loss rates through the  $\text{N}_2\text{O}_5$  heterogeneous reaction and the  $\text{NO}$  reaction ~~werewas believed to be~~ kept in balance with the  $\text{NO}_3$  production rate increased by  $\text{NO}_2$  concentrations. At high  $\text{NO}_x$  conditions, the ratios sensitively decreased with the increase of  $\text{NO}_x/\text{NO}_x$  concentrations, which is explained ~~thatby~~ the increase of  $\text{NO}_3$  loss rates by  $\text{NO}$ , resulting in a decline in the ratios.

带格式的: 段落间距段前: 0 磅, 段后: 0 磅

带格式的: 字体: 加粗

带格式的: 字体: 倾斜, 下标

带格式的: 字体: 倾斜, 下标

To better understand the nonlinear effect of NO<sub>2</sub> and O<sub>3</sub> on the nighttime VOC oxidation, we further explored the effect of O<sub>3</sub> concentration on the ratios existing in different concentrations of NO<sub>2</sub>. As shown in Fig. S13S15, in higher concentrations of NO<sub>2</sub>, the threshold of lower O<sub>3</sub> concentrations ~~were~~<sup>was</sup> required for the R<sub>NO<sub>3</sub></sub> to become constant, which reflected the couple ~~influence~~<sup>influences</sup> of NO<sub>2</sub> and O<sub>3</sub> on nighttime VOC oxidation through the nonlinear response, and indicated that in the environment richen in NO<sub>2</sub>, nocturnal NO<sub>3</sub> chemistry easily tended to be more dominant.

#### 4. Conclusions and implications

In this study, we showed ~~that~~ the NO<sub>3</sub> reactivity towards measured VOC highly varied with ~~strong~~<sup>big</sup> seasonal differences, ~~which was~~ mainly driven by isoprene concentrations. The top 6 contributors to the measured NO<sub>3</sub> reactivity towards VOC were isoprene, styrene, cis-2-butene, trans-2-butene, trans-2-pentene, and propylene. Among them, isoprene and styrene contributed most of the reactivity. In addition, monoterpenes are proposed to be a significant source of NO<sub>3</sub> reactivity. Recently studies showed ~~the~~<sup>that</sup> anthropogenic emissions ~~contributes~~<sup>contribute</sup> significantly to the ambient MNTs concentrations ~~by~~<sup>through</sup> biomass burning, traffic and volatile chemical product emissions in the urban regions, it would further enhance the importance of nocturnal NO<sub>3</sub> oxidation (Coggon et al., 2021; Nelson et al., 2021; Peng et al., 2022; Qin et al., 2020; Wang et al., 2022). It should be noted that the estimated contributions of MNTs only considered the biogenic emissions and may ~~be~~ represent the lower bias, ~~thus~~. <sup>Thus</sup> we highlight the importance of field observation of MNTs for advancing the understanding the nighttime NO<sub>3</sub> chemistry. In addition, it should be noted that we didn't take the contributions of OVOC into account, since the reaction rate coefficients of OVOC with NO<sub>3</sub> are small (Ambrose et al., 2007).

Looking <sup>for</sup> insight to the trend and evolution of detailed NO<sub>3</sub> chemistry is very scare, but it can ~~really~~<sup>be</sup> helpful to understand <sup>the</sup> response of the nocturnal chemistry on the emission change at a large time scale. Limited by the non-extensive and non-continuous observation, we cannot obtain the long-time measurement of all the VOC species in multiple sites. Since isoprene and styrene are good indicators of NO<sub>3</sub> reactivity in different seasons, at least as we ~~shows~~<sup>showed</sup> in urban Beijing, those can be used to estimate the NO<sub>3</sub> reactivity towards VOC to reestablish the long-term trend of NO<sub>3</sub> reactivity in urban regions for further evaluation of its history of nighttime chemistry. We admitted that the estimation of <sup>the</sup> NO<sub>3</sub> reactivity trend ~~may~~<sup>might</sup> be highly uncertain, but this attempt may be very helpful to know the level and overall change of nighttime chemistry.

We showed that NO<sub>3</sub> dominated the nighttime VOC oxidation in Beijing, but the oxidation ratio had a strong nonlinear relationship with O<sub>3</sub> and ~~NO<sub>x</sub>~~<sup>NO<sub>x</sub></sup> concentrations. With the NO<sub>2</sub> concentrations ~~decreased~~<sup>decreasing</sup>, the threshold values of O<sub>3</sub> between <sup>the</sup> sensitive regime and non-sensitive regime tended to increase, indicative of the nighttime oxidation by NO<sub>3</sub> would be more easily affected by the level of O<sub>3</sub> with the ~~implement~~<sup>implementation</sup> of sustaining NO<sub>x</sub> reduction in the future. The threshold values of O<sub>3</sub> can provide an effective basis for the measures to control nocturnal chemical and secondary organic ~~aerosols~~<sup>aerosol</sup> pollution in the typical urban region.

**Code/Data availability.** The datasets used in this study are available from the corresponding author upon request (wanghch27@mail.sysu.edu.cn; k.lu@pku.edu.cn).

带格式的: 字体: 倾斜, 下标

**Author contributions.** H.C.W. and K.D.L. designed the study. H.J.H. and H.C.W. analyzed the data with input from J.W., Z.L.Z., X.Z.X., T.Y.Z., X.R.C., X.L., ~~M.M.Q~~and ~~S.J.F.~~, ~~W.X.F.~~ provided the ~~modelled~~~~modeled~~ monoterpene and isoprene data, X.L., L.M.Z., M.H., and Y.H.Z. organized this field campaign and provided the field measurement dataset. H.J.H. and H.C.W. wrote the paper with input from K.D.L.

**Competing interests.** The authors declare that they have no conflicts of interest.

**Acknowledgments.** This project is supported by the National Natural Science Foundation of China (42175111, 21976006-), ~~the Guangdong Major Project of Basic and Applied Basic Research (grant no. 2020B0301030004), the Fundamental Research Funds for the Central Universities, Sun Yat-sen University (23lgbj002).~~ Thanks for the data contributed by ~~the~~ field campaign team.

**Reference.**

Ambrose JL, Mao H, Mayne HR, Stutz J, Talbot R, Sive BC. Nighttime nitrate radical chemistry at Appledore island, Maine during the 2004 international consortium for atmospheric research on transport and transformation. *Journal of Geophysical Research-Atmospheres* 2007; 112: 19.

Asaf D, Pedersen D, Matveev V, Peleg M, Kern C, Zingler J, et al. Long-Term Measurements of NO<sub>3</sub> Radical at a Semiarid Urban Site: 1. Extreme Concentration Events and Their Oxidation Capacity. *Environmental Science & Technology* 2009; 43: 9117-9123.

Atkinson R, Arey J. Atmospheric degradation of volatile organic compounds. *Chemical Reviews* 2003; 103: 4605-4638.

Bertram TH, Thornton JA. Toward a general parameterization of N<sub>2</sub>O<sub>5</sub> reactivity on aqueous particles: the competing effects of particle liquid water, nitrate and chloride. *Atmospheric Chemistry and Physics* 2009; 9: 8351-8363.

Brown SS. Applicability of the steady state approximation to the interpretation of atmospheric observations of NO<sub>3</sub> and N<sub>2</sub>O<sub>5</sub>. *Journal of Geophysical Research* 2003; 108.

Brown SS, Dibb JE, Stark H, Aldener M, Vozella M, Whitlow S, et al. Nighttime removal of NO<sub>x</sub> in the summer marine boundary layer. *Geophysical Research Letters* 2004; 31: 5.

Brown SS, Ryerson TB, Wollny AG, Brock CA, Peltier R, Sullivan AP, et al. Variability in nocturnal nitrogen oxide processing and its role in regional air quality. *Science* 2006; 311: 67-70.

Brown SS, Stutz J. Nighttime radical observations and chemistry. *Chemical Society Reviews* 2012; 41: 6405-6447.

Chen X, Wang H, Liu Y, Su R, Wang H, Lou S, et al. Spatial characteristics of the nighttime oxidation capacity in the Yangtze River Delta, China. *Atmospheric Environment* 2019; 208: 150-157.

Cheng X, Li H, Zhang YJ, Li YP, Zhang WQ, Wang XZ, et al. Atmospheric isoprene and monoterpenes in a typical urban area of Beijing: Pollution characterization, chemical reactivity and source identification. *Journal of Environmental Sciences* 2018; 71: 150-167.

Coggon MM, Gkatzelis GI, McDonald BC, Gilman JB, Schwantes RH, Abuhassan N, et al. Volatile chemical product emissions enhance ozone and modulate urban chemistry. *Proceedings of the National Academy of Sciences of the United States of America* 2021; 118.

Crowley JN, Schuster G, Pouvesle N, Parchatka U, Fischer H, Bonn B, et al. Nocturnal nitrogen oxides at a rural mountain-site in south-western Germany. *Atmospheric Chemistry and Physics* 2010; 10: 2795-2812.

Dentener FJ, Crutzen PJ. Reaction of N<sub>2</sub>O<sub>5</sub> on tropospheric aerosols: impact on the global distributions of NO<sub>x</sub>, O<sub>3</sub>, OH. *Journal of Geophysical Research* 1993; 98: 7149-7163.

Edwards PM, Aikin KC, Dube WP, Fry JL, Gilman JB, de Gouw JA, et al. Transition from high- to low-NO<sub>x</sub> control of nighttime oxidation in the southeastern US. *Nature Geoscience* 2017; 10: 490-+.

带格式的： 字体颜色： 自动设置

---

579 Evans MJ, Jacob DJ. Impact of new laboratory studies of N<sub>2</sub>O<sub>5</sub> hydrolysis on global model budgets of tropospheric nitrogen  
580 oxides, ozone, and OH. *Geophysical Research Letters* 2005; 32: 4.

581 Goldstein AH, Galbally IE. Known and unexplored organic constituents in the Earth's atmosphere. *Geochimica Et*  
582 *Cosmochimica Acta* 2009; 73: A449-A449.

583 Hallquist M, Stewart DJ, Stephenson SK, Cox RA. Hydrolysis of N<sub>2</sub>O<sub>5</sub> on sub-micron sulfate aerosols. *Physical Chemistry*  
584 *Chemical Physics* 2003; 5: 3453-3463.

585 Kane SM, Caloz F, Leu MT. Heterogeneous Uptake of Gaseous N<sub>2</sub>O<sub>5</sub> by (NH<sub>4</sub>)<sub>2</sub>SO<sub>4</sub>, NH<sub>4</sub>HSO<sub>4</sub>, and H<sub>2</sub>SO<sub>4</sub> Aerosols. *The*  
586 *Journal of Physical Chemistry A* 2001; 105: 6465-6470.

587 Kiendler-Scharr A, Mensah AA, Friese E, Topping D, Nemitz E, Prevot ASH, et al. Ubiquity of organic nitrates from nighttime  
588 chemistry in the European submicron aerosol. *Geophysical Research Letters* 2016; 43: 7735-7744.

589 Lee BS, Wang JL. Concentration variation of isoprene and its implications for peak ozone concentration. *Atmospheric*  
590 *Environment* 2006; 40: 5486-5495.

591 Li L, Li H, Zhang XM, Wang L, Xu LH, Wang XZ, et al. Pollution characteristics and health risk assessment of benzene  
592 homologues in ambient air in the northeastern urban area of Beijing, China. *Journal of Environmental Sciences*  
593 2014; 26: 214-223.

594 Li L, Wu F, Meng X. Seasonal and Diurnal Variation of Isoprene in the Atmosphere of Beijing. *Environmental Monitoring in*  
595 *China* 2013; 29: 120-124.

596 Liebmann J, Karu E, Sobanski N, Schuladen J, Ehn M, Schallhart S, et al. Direct measurement of NO<sub>3</sub> radical reactivity in a  
597 boreal forest. *Atmospheric Chemistry and Physics* 2018a; 18: 3799-3815.

598 Liebmann JM, Muller JBA, Kubistin D, Claude A, Holla R, Plass-Dulmer C, et al. Direct measurements of NO<sub>3</sub> reactivity in  
599 and above the boundary layer of a mountaintop site: identification of reactive trace gases and comparison with  
600 OH reactivity. *Atmospheric Chemistry and Physics* 2018b; 18: 12045-12059.

601 Liebmann JM, Muller JBA, Kubistin D, Claude A, Holla R, Plass-Dülmer C, et al. Direct measurements of  
602 NO<sub>3</sub>; reactivity in and above the boundary layer of a mountaintop site: identification of  
603 reactive trace gases and comparison with OH reactivity. *Atmospheric Chemistry and Physics* 2018c; 18: 12045-  
604 12059.

605 Liebmann JM, Schuster G, Schuladen JB, Sobanski N, Lelieveld J, Crowley JN. Measurement of ambient NO<sub>3</sub> reactivity:  
606 design, characterization and first deployment of a new instrument. *Atmospheric Measurement Techniques* 2017;  
607 10: 1241-1258.

608 Mao J, Li L, Li J, Sulaymon ID, Xiong K, Wang K, et al. Evaluation of Long-Term Modeling Fine Particulate Matter and Ozone  
609 in China During 2013–2019. *Frontiers in Environmental Science* 2022; 10.

610 Meng X, Hu EJ, Li XT, Huang ZH. Experimental and kinetic study on laminar flame speeds of styrene and ethylbenzene.  
611 *Fuel* 2016; 185: 916-924.

612 Miller RR, Newhook R, Poole A. Styrene production, use and human exposure. *Critical Reviews in Toxicology* 1994; 24: S1-  
613 S10.

614 Mogel I, Baumann S, Bohme A, Kohajda T, von Bergen M, Simon JC, et al. The aromatic volatile organic compounds toluene,  
615 benzene and styrene induce COX-2 and prostaglandins in human lung epithelial cells via oxidative stress and p38  
616 MAPK activation. *Toxicology* 2011; 289: 28-37.

617 Nelson BS, Stewart GJ, Drysdale WS, Newland MJ, Vaughan AR, Dunmore RE, et al. In situ ozone production is highly  
618 sensitive to volatile organic compounds in Delhi, India. *Atmospheric Chemistry and Physics* 2021; 21: 13609-  
619 13630.

620 Ng NL, Brown SS, Archibald AT, Atlas E, Cohen RC, Crowley JN, et al. Nitrate radicals and biogenic volatile organic  
621 compounds: oxidation, mechanisms, and organic aerosol. *Atmospheric Chemistry and Physics* 2017; 17: 2103-  
622 2162.

---

623 Osthoff HD, Roberts JM, Ravishankara AR, Williams EJ, Lerner BM, Sommariva R, et al. High levels of nitryl chloride in the  
624 polluted subtropical marine boundary layer. *Nature Geoscience* 2008; 1: 324-328.

625 Peng Y, Mouat AP, Hu Y, Li M, McDonald BC, Kaiser J. Source appointment of volatile organic compounds and evaluation  
626 of anthropogenic monoterpene emission estimates in Atlanta, Georgia. *Atmospheric Environment* 2022; 288.

627 Qin M, Murphy BN, Isaacs KK, McDonald BC, Lu Q, McKeen SA, et al. Criteria pollutant impacts of volatile chemical  
628 products informed by near-field modelling. *Nature Sustainability* 2020; 4: 129-137.

629 Radica F, Della Ventura G, Malfatti L, Guidi MC, D'Arco A, Grilli A, et al. Real-time quantitative detection of styrene in  
630 atmosphere in presence of other volatile-organic compounds using a portable device. *Talanta* 2021; 233: 7.

631 Riba ML, Tathy JP, Tsiropoulos N, Monsarrat B, Torres L. Diurnal variation in the concentration of  $\alpha$ - and  $\beta$ -pinene in the  
632 landes forest (France). *Atmospheric Environment* 1987; 21: 191-193.

633 Schaeffer V, Bhooshan B, Chen S, Sonenthal J, Hodgson A. Characterization of Volatile Organic Chemical Emissions From  
634 Carpet Cushions. *Journal of the Air & Waste Management Association* (1995) 1996; 46: 813-820.

635 Stark H, Lerner BM, Schmitt R, Jakoubek R, Williams EJ, Ryerson TB, et al. Atmospheric in situ measurement of nitrate  
636 radical (NO<sub>3</sub>) and other photolysis rates using spectroradiometry and filter radiometry. *Journal of Geophysical  
637 Research-Atmospheres* 2007; 112: 11.

638 Stutz J, Wong KW, Lawrence L, Ziemba L, Flynn JH, Rappengluck B, et al. Nocturnal NO<sub>3</sub> radical chemistry in Houston, TX.  
639 *Atmospheric Environment* 2010; 44: 4099-4106.

640 Tan ZF, Fuchs H, Lu KD, Hofzumahaus A, Bohn B, Broch S, et al. Radical chemistry at a rural site (Wangdu) in the North  
641 China Plain: observation and model calculations of OH, HO<sub>2</sub> and RO<sub>2</sub> radicals. *Atmospheric Chemistry and  
642 Physics* 2017; 17: 663-690.

643 Tang WC, Hemm I, Eisenbrand G. Estimation of human exposure to styrene and ethylbenzene. *Toxicology* 2000; 144: 39-  
644 50.

645 Vrekoussis M, Mihalopoulos N, Gerasopoulos E, Kanakidou M, Crutzen PJ, Lelieveld J. Two-years of NO<sub>3</sub> radical  
646 observations in the boundary layer over the Eastern Mediterranean. *Atmospheric Chemistry and Physics* 2007;  
647 7: 315-327.

648 Wang H, Lu K, Chen X, Zhu Q, Chen Q, Guo S, et al. High N<sub>2</sub>O<sub>5</sub> Concentrations Observed in Urban Beijing: Implications of  
649 a Large Nitrate Formation Pathway. *Environmental Science & Technology Letters* 2017a; 4: 416-420.

650 Wang H, Lu K, Guo S, Wu Z, Shang D, Tan Z, et al. Efficient N<sub>2</sub>O<sub>5</sub> uptake and NO<sub>3</sub> oxidation in the outflow of urban Beijing.  
651 *Atmospheric Chemistry and Physics* 2018a; 18: 9705-9721.

652 Wang H, Ma X, Tan Z, Wang H, Chen X, Chen S, et al. Anthropogenic monoterpenes aggravating ozone pollution. *National  
653 Science Review* 2022.

654 Wang H, Wang H, Lu X, Lu K, Zhang L, Tham YJ, et al. Increased night-time oxidation over China despite widespread  
655 decrease across the globe. *Nature Geoscience* 2023.

656 Wang HC, Lu KD, Chen SY, Li X, Zeng LM, Hu M, et al. Characterizing nitrate radical budget trends in Beijing during 2013-  
657 2019. *Science of the Total Environment* 2021; 795: 9.

658 Wang HC, Lu KD, Guo S, Wu ZJ, Shang DJ, Tan ZF, et al. Efficient N<sub>2</sub>O<sub>5</sub> uptake and NO<sub>3</sub> oxidation in the outflow of urban  
659 Beijing. *Atmospheric Chemistry and Physics* 2018b; 18: 9705-9721.

660 Wang HC, Lu KD, Tan ZF, Sun K, Li X, Hu M, et al. Model simulation of NO<sub>3</sub>, N<sub>2</sub>O<sub>5</sub> and ClNO<sub>2</sub> at a rural site in Beijing during  
661 CAREBeijing-2006. *Atmospheric Research* 2017b; 196: 97-107.

662 Wayne RP, Barnes I, Biggs P, Burrows JP, Canosa-Mas CE, Hjorth J, et al. The nitrate radical: physics, chemistry, and the  
663 atmosphere. *Atmospheric Environment, Part A (General Topics)* 1991; 25A: 1-203.

664 Wu K, Yang X, Chen D, Gu S, Lu Y, Jiang Q, et al. Estimation of biogenic VOC emissions and their corresponding impact on  
665 ozone and secondary organic aerosol formation in China. *Atmospheric Research* 2020; 231.

666 Wu L, Sun Y, Tian Y, Su D. Composition Spectrum of Biogenic Volatile Organic Compounds Released by Typical Flowers in

Beijing. Environmental Science and Technology 2014; 37: 154-158.

Xia C, Xiao L. Estimation of biogenic volatile organic compounds emissions in Jing-Jin-Ji. *Acta Scientiae Circumstantiae* 2019; 39: 2680-2689.

Yang Y, Wang YH, Zhou PT, Yao D, Ji DS, Sun J, et al. Atmospheric reactivity and oxidation capacity during summer at a suburban site between Beijing and Tianjin. *Atmospheric Chemistry and Physics* 2020; 20: 8181-8200.

Yuan ZB, Lau AKH, Shao M, Louie PKK, Liu SC, Zhu T. Source analysis of volatile organic compounds by positive matrix factorization in urban and rural environments in Beijing. *Journal of Geophysical Research-Atmospheres* 2009; 114: 14.

Zhu J, Wang S, Zhang S, Xue R, Gu C, Zhou B. Changes in NO<sub>3</sub> Radical and Its Nocturnal Chemistry in Shanghai From 2014 to 2021 Revealed by Long - Term Observation and a Stacking Model: Impact of China's Clean Air Action Plan. *Journal of Geophysical Research: Atmospheres* 2022; 127.

Zielinska B, Sagebiel JC, Harshfield G, Gertler AW, Pierson WR. Volatile organic compounds up to C-20 emitted from motor vehicles; Measurement methods. *Atmospheric Environment* 1996; 30: 2269-2286.

Zilli M, Palazzi E, Sene L, Converti A, Del Borghi M. Toluene and styrene removal from air in biofilters. *Process Biochemistry* 2001; 37: 423-429.

Zou Y, Deng X, Li F, Wang B, Tan H, Deng T, et al. Variation characteristics, chemical reactivity and sources of isoprene in the atmosphere of Guangzhou. *Acta Scientiae Circumstantiae* 2015; 35: 647-655.